

# Nanoscale

Accepted Manuscript



This is an *Accepted Manuscript*, which has been through the Royal Society of Chemistry peer review process and has been accepted for publication.

*Accepted Manuscripts* are published online shortly after acceptance, before technical editing, formatting and proof reading. Using this free service, authors can make their results available to the community, in citable form, before we publish the edited article. We will replace this *Accepted Manuscript* with the edited and formatted *Advance Article* as soon as it is available.

You can find more information about *Accepted Manuscripts* in the [Information for Authors](#).

Please note that technical editing may introduce minor changes to the text and/or graphics, which may alter content. The journal's standard [Terms & Conditions](#) and the [Ethical guidelines](#) still apply. In no event shall the Royal Society of Chemistry be held responsible for any errors or omissions in this *Accepted Manuscript* or any consequences arising from the use of any information it contains.

## ARTICLE

# Shape-Controllable and Versatile Synthesis of Copper Nanocrystals with Amino Acids as Capping Agents

Cite this: DOI: 10.1039/x0xx00000x

Jin-Cheng Yu,<sup>a, b</sup> Fu-Gang Zhao,<sup>\*a, b</sup> Wei Shao,<sup>a, b</sup> Cong-Wu Ge<sup>b</sup> and Wei-Shi Li<sup>\*a, b</sup>Received 00th January 2014,  
Accepted 00th January 2014

DOI: 10.1039/x0xx00000x

[www.rsc.org/](http://www.rsc.org/)

Thanks to their outstanding properties and a wide range of promising applications, the development of a versatile and convenient preparation method for metallic copper nanocrystals with controllable shape is of primary significance. Different from literature work that utilized a capping agent bearing only one single kind of Cu binding functionality, either amino or carboxylic, for their preparation and shape control, this contribution reports a convenient method to engage both amino and carboxylic binding units at the same time. In this method, natural amino acids have been chosen as capping agents and demonstrated their versatile capabilities for the preparation of both Cu nanoparticles and nanowires. Detail X-ray photoelectron spectroscopy revealed that the binding mode between amino acids and Cu surface is highly dependent on their chemical structures. Of interest, the produced Cu nanocrystals, exhibited extraordinarily excellent anti-oxidation power. Furthermore, it was found that the multiple functionalities of amino acids not only bring a great impact on the properties of the capped nanocrystals, such as solvent dispersibility, but also provide a convenient route for their further modification and functionalization.

## Introduction

Copper nanomaterials, including nanowires (CuNWs) and nanoparticles (CuNPs), have received significant attention due to their excellent optical, electrical, catalytic, and antifungal properties, and a wide range of potential applications in the fields of catalysis,<sup>1</sup> opto-electronics,<sup>2</sup> chemical sensors,<sup>3, 4</sup> and biomedicines and biotechnologies.<sup>5, 6</sup> Particularly, as compared with Ag, the best electrically conducting metal, Cu is only 6% less conductive, but 1000 times more abundant and 100 times less expensive.<sup>7</sup> This makes Cu nanomaterials extraordinarily attractive to replace Ag counterparts for printable conducting inks and films. Encouraged by such merits and promising applications, researchers have made great effort in the past decades to find an easy and low cost way for their preparation. Several methods have been successfully established, including wet chemical reduction,<sup>8–19</sup> chemical vapor depositions,<sup>20</sup> template-assisted syntheses,<sup>21, 22</sup> and electronic deposition technologies.<sup>23</sup> Among these methods, the first one has been regarded as one of the most feasible ways since it is versatile in nanostructure control and easy to scale up in low cost. In such a method, a Cu salt precursor is reduced by a reductive agent (e.g. hydrazine) in an aqueous or non-aqueous media in the presence of a surfactant<sup>18</sup> or capping agent.<sup>11–13</sup> Here, the surfactant/capping agent is vitally important since it determines the nanostructure of the final product and avoids them agglomerate into big species. Surfactants generally form

micelles and provide a special nanoscale microenvironment different from bulk media for growing nanoparticles and nanorods. In contrast, capping agents possess certain Cu coordination units, which can bind onto Cu surface and thus stabilize Cu nanocrystals from agglomeration. More importantly, the binding may prefer certain facets of Cu nanocrystals and cause preferential growth into anisotropic nanostructures, like nanowires. To date, there are two kinds of capping agents, amines<sup>9–15, 24</sup> and carboxylic acids,<sup>16, 17</sup> have been reported. Amino-functionalized agents, such as ethylenediamine (EDA),<sup>11–14</sup> hexadecylamine (HDA)<sup>9, 10</sup> and oleylamine,<sup>21</sup> were mainly engaged in the synthesis of CuNWs. It was reported that amino unit can preferentially bind to the side facets of CuNWs and cause preferential Cu crystal growth along the axial [110] direction.<sup>22</sup> However, when carboxylic acids, such as oleic acid,<sup>17</sup> lactic acid and glycolic acid,<sup>16</sup> were chosen as capping agents, CuNPs were generated. These results may suggest that carboxylic acid binds to all the facets of Cu nanocrystals non-selectively. Here, one curious question is arising: if capping molecules carry both amino and carboxylic units, what will happen?

With such a question in mind, we recently endeavored to study amino acids as capping agents for Cu nanocrystal preparation. Amino acids are ubiquitous natural substances bearing both amino and carboxylic functionalities in one molecule. We tested 17 of 20 natural amino acids (Fig. 1) and found most of them are versatile in the synthesis of Cu

nanomaterials. According to structural differences in their  $\alpha$ -substituents, these amino acids can be roughly categorized into four groups: (1) those R-substituents carrying only C and H elements, either aliphatic or aromatic, (2) those R-substituents bearing a hydroxyl or thiol unit, (3) those R-substituents bearing a carboxylic unit or its amide derivative, and (4) those R-substituents containing an additional N-binding site. We found these different  $\alpha$ -substituent structures have great impact on the shape, dimension, and properties of the resultant Cu nanocrystals. Furthermore, we found that amino acids as coating agents can greatly improve the anti-oxidation property and water dispersibility of the resultant Cu nanomaterials, which are very important for their real applications.

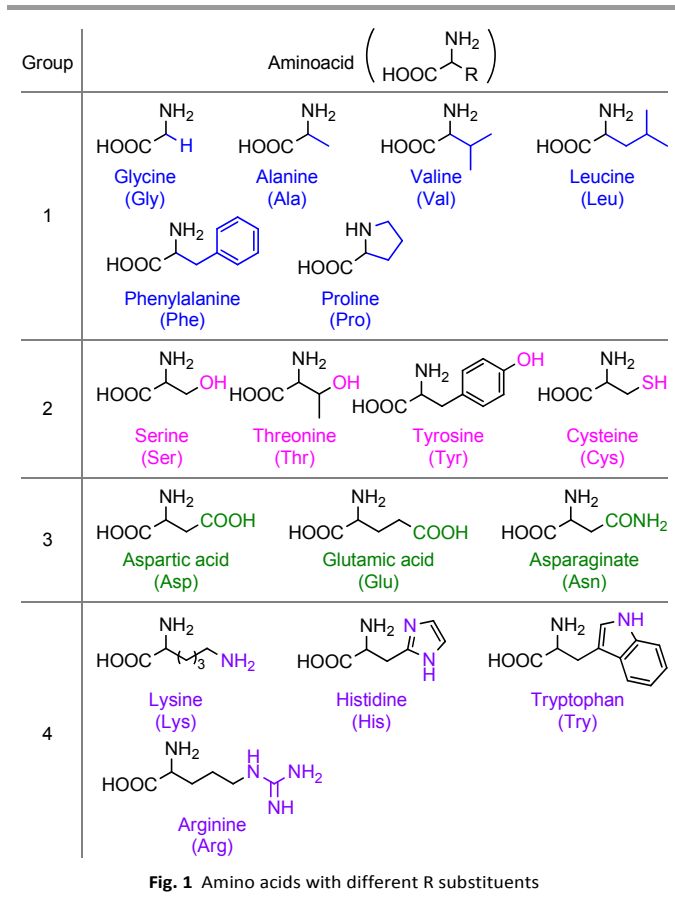


Fig. 1 Amino acids with different R substituents

## Experimental Section

### General procedure for synthesis of Cu nanomaterials

Copper nanomaterials were synthesized by chemical reduction of copper ions in alkaline solution with amino acids as capping agents. In a typical procedure, an aqueous NaOH solution ( $15 \text{ mol L}^{-1}$ , 40 mL, 600 mmol) was added with an aqueous copper nitrate solution ( $0.1 \text{ mol L}^{-1}$ , 2 mL, 0.2 mmol), the desired amino acid ( $3.72 \text{ mmol}$ ) and subsequently a hydrazine solution (35 wt%, 50  $\mu\text{L}$ , 0.55 mmol). Then, the reaction mixture was gently stirred at  $80 \text{ }^\circ\text{C}$ . A quick color change, from blue to white then to brick-red, was observed within 15 min. Meanwhile, the reddish Cu nanocrystals started to generate and

float in the upper layer of the reaction mixture. After 30 min, the resulted suspension was filtered over  $0.22 \mu\text{m}$  nylon membrane. The filter cake was carefully washed with a large amount of deionized water and dried in vacuum oven, affording red copper nanocrystal powder.

### Characterization methods

The morphology and sizes of Cu nanocrystals were characterized by field emission scanning electron microscopy (FE SEM) on a Hitachi S-4800 instrument. Transmission electron microscopy (TEM) and selected area electron diffraction (SAED) were performed on FEI Tecnai G2 Spher microscopes operated at 200 kV. Samples were prepared by placing a drop of very dilute aqueous dispersion on a holey carbon-coated copper grid and dried at ambient condition. Crystal structures were determined by powder X-ray diffraction (XRD) using a PANalytical X'Pert Pro MPD diffractometer with Cu- $K\alpha$  radiation. X-ray photoelectron spectroscopy (XPS) was carried out on a PHI-5000 VersaProbe photoelectron spectrometer under  $10^{-7} \text{ Pa}$  using monochromatic Al  $K\alpha$  X-ray excitation source operating at 100 W. Thermogravimetric analysis (TGA) was carried out on a Shimadzu DTG-60 thermal gravimetric analyzer with a heating rate of  $10 \text{ }^\circ\text{C min}^{-1}$  under a nitrogen flow.

## Results and discussion

The preparation of Cu nanocrystals followed the same procedure reported by Wiley *et al.*,<sup>12</sup> but using an amino acid to replace EDA as the capping agent. That is, a Cu salt precursor ( $\text{Cu}(\text{NO}_3)_2$  in our work) was reduced by hydrazine in the presence of a desired amino acid capping agent in a concentrated NaOH aqueous media. We found both CuNWs and CuNPs could be prepared by this approach. For example when glycine was used as the capping agent and the reaction was carried out under the conditions of  $\text{Cu}(\text{NO}_3)_2$  (4.76 mM), NaOH (3000 eq.), glycine (18.6 eq.) and  $\text{N}_2\text{H}_4 \cdot \text{H}_2\text{O}$  (2.75 eq.) at  $80 \text{ }^\circ\text{C}$ , Cu nanowires were produced predominately (Fig. 2a and 2c). The length of the nanowires was  $21.2 \pm 3.9 \mu\text{m}$ , while their diameter was  $301 \pm 50 \text{ nm}$ . Although the CuNWs appeared homogenous and smooth in SEM, their surface is somewhat rough, as revealed by TEM (Fig. 2e). The selected area electron diffraction (SAED) disclosed CuNWs have a single-crystalline structure. In the XRD profile, only three peaks  $43.3$ ,  $50.5$  and  $74.1^\circ$  were clearly observed (Fig. 2g). These peaks could be indexed to (111), (200) and (220) diffraction of a face-centered cubic (fcc) crystal structure of copper phase.<sup>25</sup> No other phase, such as  $\text{Cu}_2\text{O}$  and  $\text{CuO}$ ,<sup>10, 16, 17</sup> was detected, indicating the generated CuNWs are in pure metallic state. When histidine was used as the capping agent, CuNPs were produced preferentially (Fig. 2b and 2d). The nanoparticle size was not homogeneous, with a diameter of  $2470 \pm 620 \text{ nm}$ . Although their pure metallic state was confirmed by XRD (Fig. 2h), these nanoparticles are polycrystalline, as revealed by SAED (Fig. 2f).

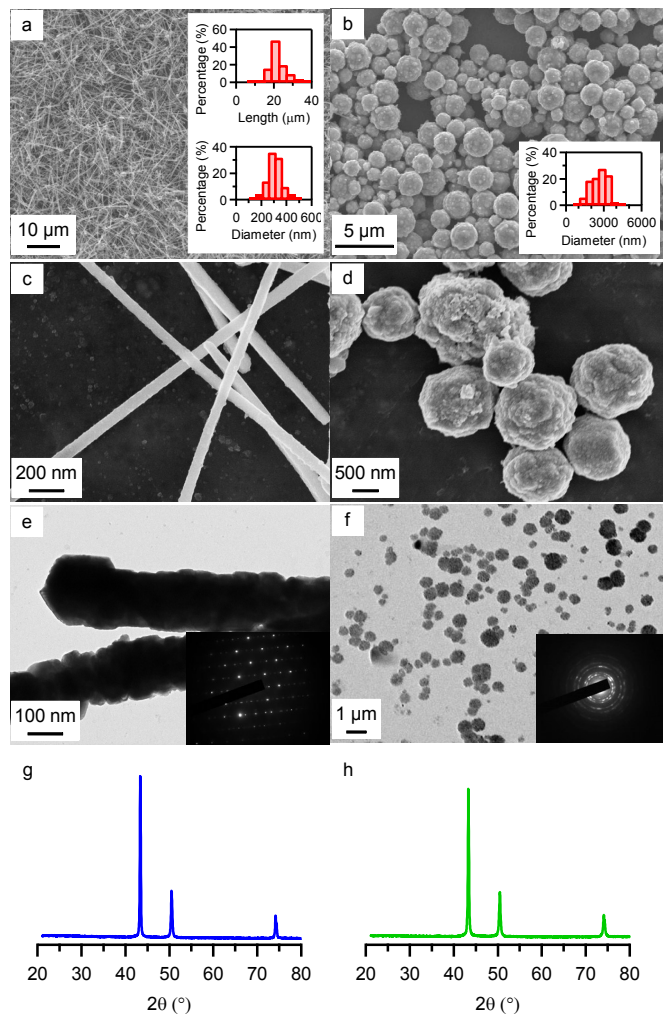


**Fig. 2** (a-d) SEM, (e, f) TEM images and (g, h) XRD profiles of (a, c, e, g) CuNW and (b, d, f, h) CuNP prepared with glycine and histidine respectively. Other conditions:  $\text{Cu}(\text{NO}_3)_2$  (4.76 mM), NaOH (3000 eq.), amino acid (18.6 eq.), and  $\text{N}_2\text{H}_4 \cdot \text{H}_2\text{O}$  (2.75 eq.) at 80 °C. Insets in (e) and (f) show their SAED patterns. Insets in (a) and (b) show their diameter and length distributions.

Besides glycine and histidine, we tested other 15 natural amino acids as the capping agent (Fig. 1) and found that their R substituents have great impact on the resultant Cu nanostructures. In group 1, glycine, alanine, valine and leucine have similar saturated aliphatic R substituents, but with an increasing size and bulky volume. When these amino acids were used as capping agents under the same conditions as those of glycine, the produced Cu nanostructures changed from long and homogeneous nanowires (glycine, Fig. 2a), to shorter nanowires (alanine, Fig. 3a), then to hedgehog-like nanostructure with several rods growing on a particle (valine, Fig. S1a) and to the predominate nanoparticles mixed with nanorods (leucine, Fig. S1b). Meanwhile, CuNPs were created in the case of phenylalanine as the capping agent, which R substituent contains a bulky phenyl unit. Of interest, nanowires grew again using proline capping agent, which has an annular and less bulk aliphatic R substituent. These examples clearly show that the size of R substituents greatly affect the final nanostructure of the product. In general, bulky R unit would

exert a large steric hindrance and then suppress the growth of Cu nanocrystals into anisotropic nanostructure, like nanowire.

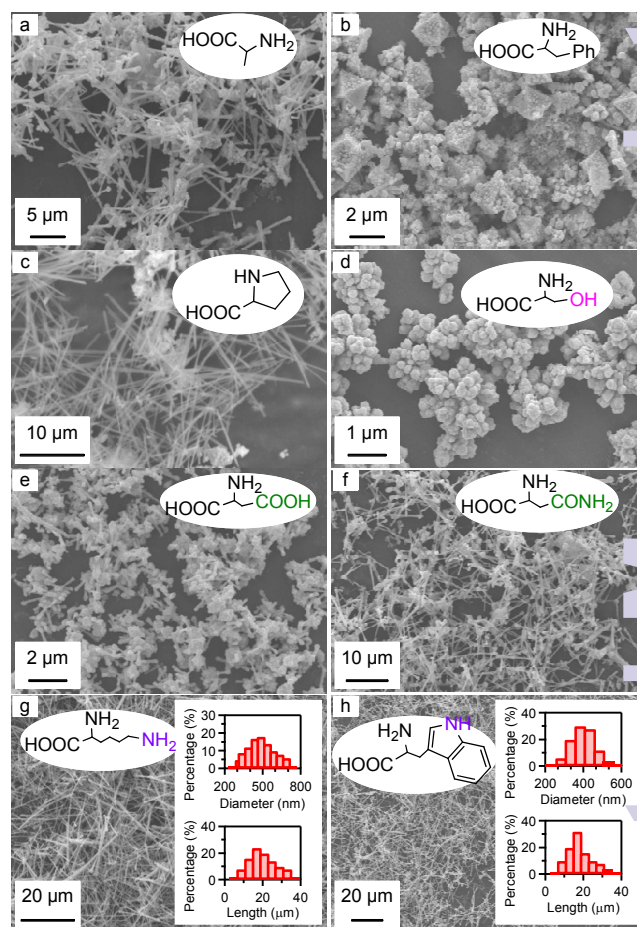


**Fig. 3** SEM images of Cu nanostructures prepared with different amino acid capping agents under the conditions of  $\text{Cu}(\text{NO}_3)_2$  (4.76 mM), NaOH (3000 eq.), amino acid (18.6 eq.), and  $\text{N}_2\text{H}_4 \cdot \text{H}_2\text{O}$  (2.75 eq.) at 80 °C. Insets in (g) and (h) show their diameter and length distributions.

Group 2 amino acids, including serine, threonine, tyrosine, and cysteine, possess one hydroxyl or thiol functional unit at the end of their R substituents. When serine, threonine and tyrosine were individually employed as the capping agent, only CuNPs were produced (Fig. 3d, S1c and S1d). However, cysteine with a thiol unit did not afford any precipitation in the reaction, suggesting it is unable to be a capping agent. Aspartic acid, glutamic acid and asparagine were classed into group 3 since all these three amino acids have a carboxylic acid or its derived group in their R substituents. Short nanorods together with nanoparticles were obtained with either aspartic acid or glutamic acid as the capping agent (Fig. 3e and S1e). When aspartic acid was changed to its amide, the longer nanowires were generated (Fig. 3f). In the case of group 4, lysine, histidine, tryptophan and arginine possess a nitrogen-containing functionality in their R substituents. Lysine has an additional primary amino functional unit and was proved to be able for the preparation of CuNWs with a diameter of  $467 \pm 105$  nm and a length of  $19.1 \pm 6.8$   $\mu\text{m}$  (Fig. 3g). Both histidine and

tryptophan possess an aza- aromatic ring, but showed different capping behavior in the reaction. Histidine predominately produced nanoparticles under the standard conditions (Fig. 2b), while tryptophan created good nanowires with a diameter of  $388 \pm 58$  nm and a length of  $17.7 \pm 6.3$   $\mu\text{m}$  (Fig. 3h). Unfortunately, like cysteine, arginine did not produce any Cu nanostructure. Thus, among the 17 tested amino acids, only cysteine and arginine did not afford any Cu nanocrystal, even other reaction conditions were changed. In fact, no color change was observed during their experiments. This implies a possible reason for their failure, that is, the strong binding of thiol/guanidine to  $\text{Cu}^{2+}$  ions significantly altered their redox potential and prevent them to be reduced by hydrazine. All these experiments clearly demonstrated that the functionality in the R substituent of the amino acid plays an important role to determine the morphology and size of the resultant Cu nanostructures.

In addition to amino acid type, other conditions, including the amount of hydrazine, NaOH concentration, and reaction temperature, were found having significant influence on the shape of the resultant Cu nanocrystals. In the case of glycine as the capping agent, the reduction of hydrazine amount to a half resulted in shorter Cu nanowires together with an increased amount of nanoparticles (Fig. S2). But when hydrazine amount was increased by a half part, nanoparticles predominately produced. The influence of NaOH concentration was not as significant as that of hydrazine (Fig. S3). Either reduction to a half or increment by a half part led to the generation of shorter nanowires (Fig. S4). And, we also found nanoparticles were predominately produced when the reaction was carried out at  $60$   $^{\circ}\text{C}$  (Fig. S5). But when reaction temperature was raised over  $70$   $^{\circ}\text{C}$ , the most generated Cu nanostructures were nanowires. Thus for glycine as the capping agent, the optimized conditions for producing Cu nanowires can be concluded as followings:  $\text{Cu}(\text{NO}_3)_2$  (4.76 mM), NaOH (3000 eq.), glycine (18.6 eq.) and  $\text{N}_2\text{H}_4 \cdot \text{H}_2\text{O}$  (2.75 eq.) at  $80$   $^{\circ}\text{C}$ . Under these conditions, we investigated the evolution of Cu nanostructures during the reaction for further understanding on their growing mechanism (Fig. S6). The initial color of the reaction mixture containing glycine, NaOH, and  $\text{Cu}(\text{NO}_3)_2$  was deep blue and turned to white and translucent after the addition of hydrazine. No precipitation happened during this procedure. After stirring at  $80$   $^{\circ}\text{C}$  for 10 min, the reaction mixture was changed to pink and turbid. The sampling found the generation of octahedron-like nanoparticles. When the reaction was further carried out for 7 min, the reaction mixture was changed to brick-red and more turbid. Both nanowires and nanoparticles were observed during this stage. After another 5 min, bronze precipitations, which are mainly nanowires, appeared and spontaneously floated at air-water interface. These experiments clearly indicated that nanowires are growing from nanoparticles during the reaction. This finding is not surprising since Wiley *et al.* also observed the same phenomena in their work.<sup>15</sup>

The so-prepared Cu nanostructures were coated with a layer of amino acids on their surface, as confirmed by TGA and XPS. For example, the 1s core level signals of carbon, nitrogen and

oxygen elements all appeared in the XPS spectrum of Gly@CuNW around 284, 400, and 530 eV, respectively (Fig. 4a). These signals unambiguously originated from the coated glycine molecules. TGA revealed that the glycine loading amount was about 3% (Fig. S7). In addition to the above bound glycine signals, the XPS spectrum of Gly@CuNW also displayed photoemission peaks from Cu electrons at 75.0 (Cu 3p), 122.0 (Cu 3s), 932.0 (Cu 2p 3/2) and 952.0 eV (Cu 2p 1/2). All these peaks are symmetrical. Furthermore, the peak of Cu<sup>+</sup> which appeared at 932.6 eV in literature,<sup>16</sup> did not show up this time. These results demonstrate the produced Cu nanomaterials are in pure Cu(0) form and free of copper oxides. The same data and phenomena were observed in the case of His@CuNW except the histidine loading amount changed to 2% (Fig. S8).

The coordination binding to nanostructure surface through their functionalities is an important feature for capping agents and plays a vital role in the shape control on the generated nanostructure. In order to get insight of these binding events in amino acid-capped Cu nanocrystals, detailed XPS analyses were performed on 1s core level signals of carbon, oxygen and nitrogen elements for the selected representative examples: glycine, serine, aspartic acid, lysine and tryptophan (Fig. 4b–f and Table 1) with a special attention paid on their changes between the free and bound forms.

As shown in Fig. 4b and Table 1, free glycine molecules displayed C 1s signals at 285.5 and 287.8 eV for their  $\text{C}-\text{NH}_2$  and  $\text{COO}^-$  moieties, respectively, while the component at 284.8 eV was coming from unexpected carbon contaminants.<sup>26–28</sup> In comparison, Gly@CuNW showed C 1s signals at 284.8, 286.7 and 287.8 eV, which are assignable to bound  $\text{C}-\text{NH}_2-\text{Cu}$  and  $\text{COO}-\text{Cu}$ , and the residue non-bounded  $\text{COO}^-$ . Clearly, the binding leads to the downshift of C 1s signals and the dramatic decrease in  $\text{COO}^-$  peak intensity, suggesting both amino and carboxylic units are in coordination state. This can be further proved by N and O 1s XPS signal changes, in which the downshift of N 1s peak (from 400.7 eV to 399.3 eV) and the splitting of O 1s signal from one peak (531.3 eV) into two (530.7 and 532.0 eV) were observed when glycine bound to Cu surface. The latter phenomenon suggests that the two oxygen atoms of carboxylic unit in free glycine are in form of  $\text{O}=\text{C}=\text{O}$  with an identical chemical surrounding, while change to the form of  $\text{C}-\text{O}-\text{Cu}$  and  $\text{C}=\text{O}$  in Gly@CuNW.<sup>16</sup> Based on the above data and analyses, the plausible binding mode for Gly@CuNW can be suggested as follows: both amino- and carboxylic acid units are bound to the surface of CuNWs (Fig. 4g).

Compared to glycine, serine displayed a similar XPS spectrum but with a more intense C 1s peak at 285.7 eV and a new O 1s peak at 532.7 eV owing to its additional hydroxyl functional group (Fig. 4c). When it was bound to Cu surface, downshifts in C (from 285.7 and 287.6 eV to 284.8 and 286.7 eV, respectively) and N (from 400.3 eV to 399.5 eV) 1s signals were observed, similar to the case of Gly@CuNW. Moreover, the O 1s XPS signals of Ser@CuNP can be fitted into three components at 530.6, 532.1 and 532.8 eV, assignable to  $\text{C}-\text{O}-\text{Cu}$ ,  $\text{C}=\text{O}$ , and non-bound  $\text{C}-\text{OH}$ . All these observations

suggest the binding mode of Ser@CuNP is the same as that of Gly@CuNW, in which amino and carboxylic acid are bound to the surface of CuNPs while the hydroxyl unit does not (Fig. 4g).

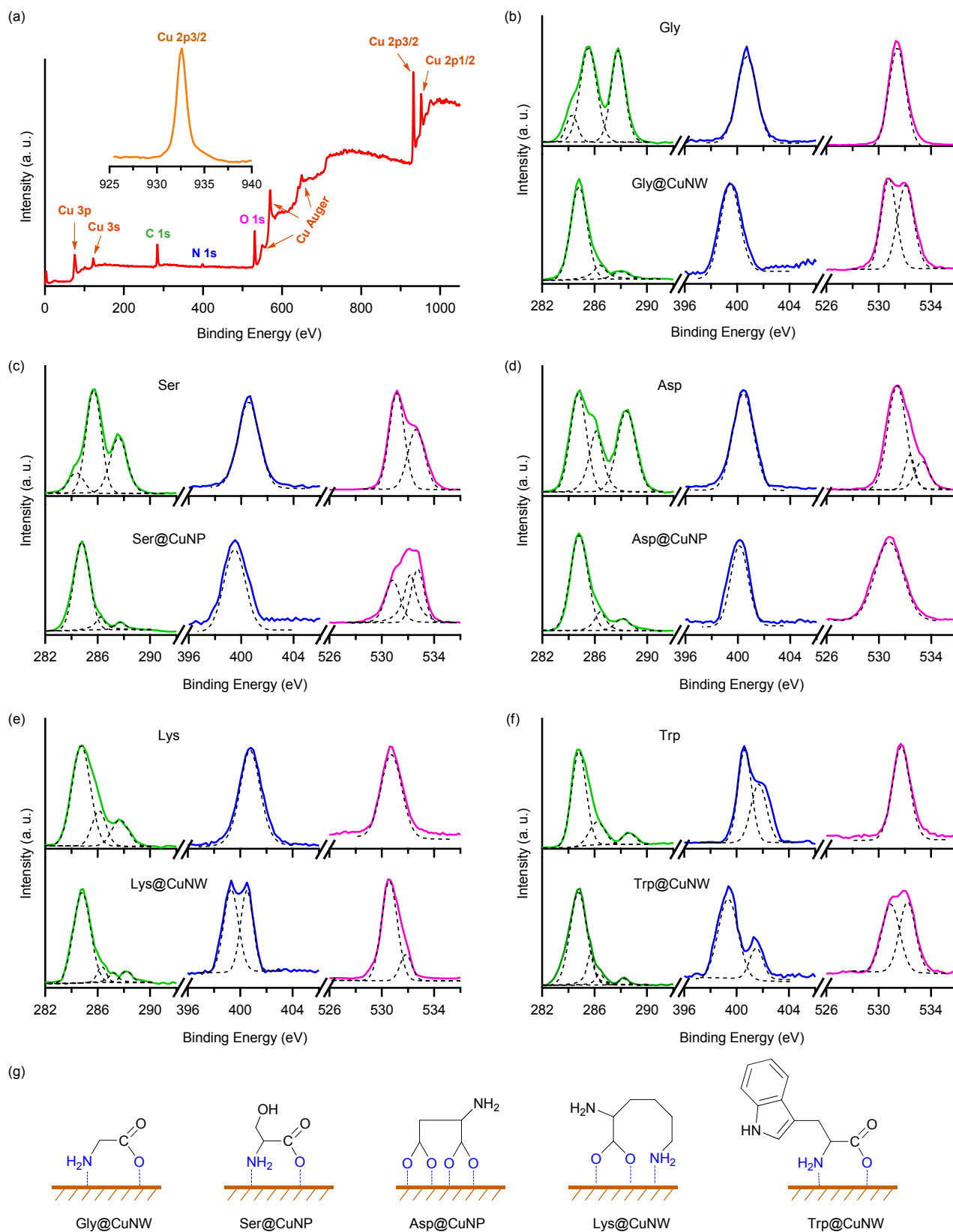


**Fig. 4** (a) Survey XPS spectrum of Gly@CuNW and curve-fitted C (green), N (blue) and O (magenta) 1s peaks of (c) glycine and Gly@CuNW, (c) serine and Ser@CuNP, (d) aspartic acid and Asp@CuNP, (e) lysine and Lys@CuNW, and (f) tryptophan and Trp@CuNW. Their plausible coordination modes are shown in (g).

**Table 1** XPS 1s core level signals of carbon, nitrogen, and oxygen for free amino acids and their bound form to Cu nanostructures.

Sample	C 1s (eV)	N 1s (eV)	O 1s (eV)
Gly	284.2, <sup>a</sup> 285.5, 287.8	400.7	531.3
Gly@CuNW	284.8, 286.4, 287.8	399.4	530.7, 532.0
Ser	284.2, <sup>a</sup> 285.7, 287.6	400.3	531.1, 532.7
Ser@CuNP	284.8, 286.2, 287.7	399.5	530.8, 532.2, 532.8
Asp	284.7, 286.1, 288.4	400.4	531.5, 532.4, 533.2
Asp@CuNP	284.8, 286.4, 288.1	400.1	530.7
Lys	284.6, 286.0, 287.6	400.8	531.7
Lys@CuNW	284.8, 286.3, 287.2, 288.2	399.3, 400.5	530.6, 531.8
Trp	284.9, 286.3, 288.6	400.6, 401.6	531.7
Trp@CuNW	284.8, 285.7, 286.5, 288.3	399.3, 401.5	530.9, 532.3

<sup>a</sup> originating from contaminants

Aspartic acid has two carboxylic and one amino functionalities. In its XPS spectrum (Fig. 4d), the C 1s signals could be fitted into three components at 284.7, 286.1 and 288.4 eV. The first peak is coming from C-NH<sub>3</sub><sup>+</sup>, while the last one is assignable to both COO<sup>-</sup> and COOH. The middle component showing at 286.1 could be attributed to C\*-COOH. In the Asp@CuNP spectrum, the first component of C 1s signals remained intact while the latter two greatly decreased their intensity. Interestingly, little change was found for N 1s XPS signal between free and bound form, since both displayed a single peak around 400 eV. Furthermore, the O 1s signal of free aspartic acid can be divided into three components at 531.5, 532.4 and 533.2 eV, indicating the presence of three kinds of O atoms with different local environment. This suggests the two carboxylic functional units are in different forms, probably COO<sup>-</sup> and COOH. However, after binding to Cu surface, these three components merged into one, which appeared at 530.7 eV. All these observations strongly suggest that the binding of aspartic acid to Cu surface is through two carboxylic functional units and in a bidentate manner, as depicted in Fig. 4g. The amino functional unit of aspartic acid is free of binding and maybe available for further functionalization.

Both lysine and tryptophan possess a second N-containing functionality but in different form, *i.e.*, primary amino and indole, respectively. The C 1s XPS signals can be fitted into three components, 284.6, 286.0, and 287.6 eV for lysine, while 284.9, 286.3, and 288.6 eV for tryptophan (Fig. 4e and 4f, Table 1). The first peak in both cases originates from C-C and C=C, while the middle one assignable to C-NH<sub>3</sub><sup>+</sup> and C-NH<sub>2</sub>, and the last one to COO<sup>-</sup>. After binding, their C 1s signals became four components, 284.8, 286.3, 287.2, and 288.2 eV for Lys@CuNW, while 284.8, 285.7, 286.5 and 288.3 eV for Trp@CuNW. The big difference between these two amino acids was found in N 1s XPS signals. Lysine displayed only one N 1s peak at 400.8 eV, implying both C-NH<sub>3</sub><sup>+</sup> and C-NH<sub>2</sub> display electron photoemission at the same wavelength. In contrast, tryptophan showed two N 1s components at 400.6 and 401.6 eV. The former is assignable to C-NH<sub>3</sub><sup>+</sup>, while the latter

originates from indole N atom. After binding, the N 1s signal of Lys@CuNW became two components at 399.3 and 400.5 eV, indicating the existence of two kinds of amino units, probably bound C-NH<sub>2</sub>-Cu and non-bound C-NH<sub>2</sub> or C-NH<sub>3</sub><sup>+</sup>. In the case of Trp@CuNW, the N 1s signal of C-NH<sub>2</sub> downshifted to 399.3 eV, implying it coordinates with Cu atoms. Whereas, the N 1s signal for indole unit remained intact, disclosing its non-bound nature. For O 1s XPS signals, both lysine and tryptophan displayed only one component, indicating two O atoms are in the same environment. However, Lys@CuNW exhibited O 1s signal with a dominated component at 530.6 eV together with a small one at 531.8 eV. This implies that the binding of carboxylic functional unit in lysine is mainly through a bidentate manner, but mingles with monodentate fashion. In contrast, two components with almost the same intensity were observed for the Trp@CuNW sample, suggesting the carboxylic binding in this case is absolutely monodentate. Based on these observations and analyses, the binding modes for Lys@CuNW and Trp@CuNW could be hypothesized as following: the binding is through carboxylic and amino units, leaving one amino group of lysine and indole unit of tryptophan non-bound (Fig. 4g). The difference between these two modes is that the carboxylic binding in Lys@CuNW is mainly bidentate, while that in Trp@CuNW is monodentate.

From the above experimental results and binding model, one may conclude some useful information how R substituents in amino acids affect their binding pattern on Cu surface, and thus the shape control of generated Cu nanocrystals. First of all, it has been strongly suggested that carboxylic unit is a much stronger binding moiety than amino unit. Thus, when the second carboxylic unit is available, like in aspartic acid, the binding is accomplished by the two carboxylic units. Since such bindings to the Cu crystal facets are non-selective, Cu nanoparticles are produced. For those R does not contain stronger coordination unit than amino, such as glycine, lysine and tryptophan, both amino and carboxylic units are bound to Cu surface, resulting in probably preferential coverage on some facets of Cu nanocrystals and the production of nanowires.<sup>22</sup> Moreover, the size of R groups also has its influence, in which larger volume may require more cone-shaped space and thus prefer the generation of nanoparticles, like in the cases of valine and phenylalanine. However, it is not clear at present why nanoparticles are produced when amino acids contain a hydroxyl unit in their R groups, such as serine. It maybe accounts for the side hydroxyl unit influence the binding selectivity of amino unit to Cu facets.

Of further interest, we found the so prepared amino acid-coated Cu nanomaterials possess unusual anti-oxidative nature when stored in solid state under ambient conditions. As shown in Fig. 5a and 5b, the XRD profiles of Gly@CuNW and His@CuNP kept unchanged even after 56 days. No any sign of copper oxides appeared. However, in the case of Cu nanowires prepared with EDA as the capping agent (EDA@CuNW),<sup>10</sup> the XRD peak of Cu<sub>2</sub>O at 36.6 ° was immediately observable after

one day storage and even grew intense along the time (Fig. 5c and 5d). This fact clearly proves that amino acids provide an excellent anti-oxidation power for Cu nanomaterials and would be good for their various promising applications.

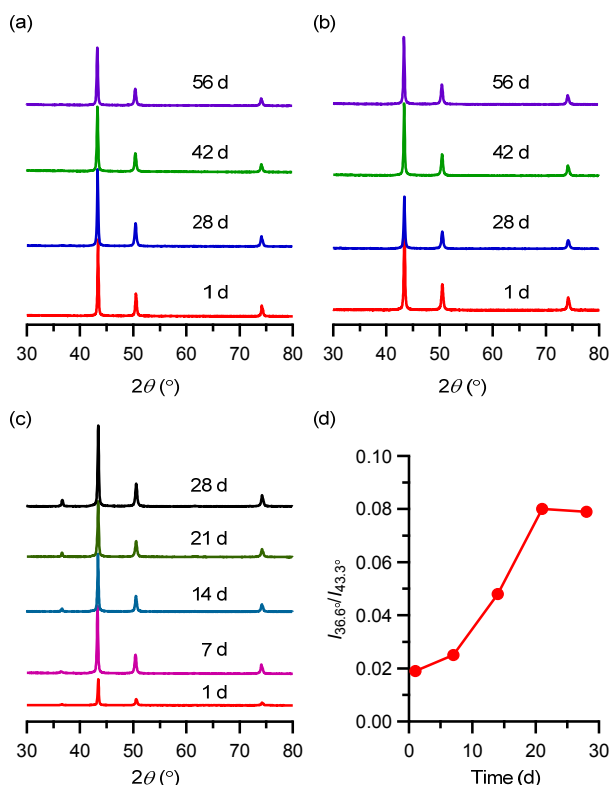


**Fig. 5** Time-dependent XRD patterns of (a) Gly@CuNW, (b) His@CuNP, and (c) EDA@CuNW stored at ambient conditions. (d) Time-dependent  $I_{36.6^\circ}/I_{43.3^\circ}$  ratio of EDA@CuNW shown in (c).

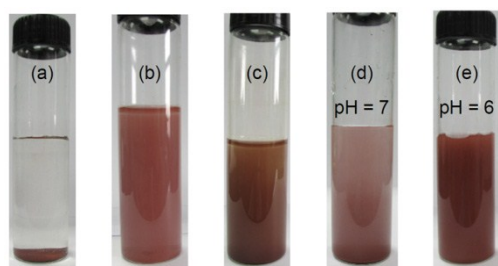


**Fig. 6** Photographs of aqueous dispersion of (a) Lys@CuNW, (b) Ser@CuNP, (c) Asp@CuNP, and (d, e) Lys@CuNW after sonication and standing for 30 min.

Furthermore, we found a great impact of amino acids on the water dispersibility of their capped Cu nanocrystals. For example, Gly@CuNW did not show any dispersibility in water (Fig. 6a). In contrast, serine, a hydroxyl-containing amino acid, enabled Cu nanoparticles standing in water with a concentration of  $0.12 \text{ mg mL}^{-1}$  after sonication and leaving undisturbed for 30 min (Fig. 6b). Such concentration was increased to  $0.27 \text{ mg mL}^{-1}$  when aspartic acid bearing an additional carboxylic unit, was used in the place of serine (Fig. 6c). Another interesting result was coming from the case of lysine capped nanowires. In neutral water (pH = 7) after sonication and leaving undisturbed for 30 min, the concentration of the dispersed Cu nanowires

was only  $0.10 \text{ mg mL}^{-1}$  (Fig. 6d). Surprisingly, such dispersibility was greatly enhanced and reached  $0.48 \text{ mg mL}^{-1}$  (Fig. 6e). According to the above binding mode analysis, Lys@CuNW has a free amino unit outward. Its protonation in acidic media could introduce additional electrostatic repulsion interactions among nanowires, and thus leads to the improvement in their dispersibility. These results indicate that multi-functionality of amino acids provides certain additional chances and methods to modify the properties of Cu nanocrystals after their generation.

## Conclusions

In this work, we have demonstrated a novel and convenient method for the preparation of Cu nanomaterials with tunable structures by using natural amino acids as capping agents. As compared with the literature methods using amines or carboxylic acids as capping agents, this amino acid approach provides the following merits and features: (1) the structural diversity of amino acids enables an easy and controllable preparation of Cu nanomaterials with a variety of nanostructures, including nanoparticles, nanorods, and nanowires; (2) the generated Cu nanocrystals possess an extraordinarily good anti-oxidation power; (3) the multiple functionalities of amino acids open a new avenue to modify and further functionalize the properties of Cu nanocrystals after their generation. Furthermore, detailed mechanical studies revealed that the binding of amino acids to Cu surface is accomplished by two functional units, one amino and one carboxylic unit in the most cases or two carboxylic units if available. This finding improves the understandings on the binding events between capping agents and Cu nanocrystals and would be valuable for their further improvement.

## Acknowledgements

We gratefully acknowledge the financial support from National Natural Science Foundation of China (Nos. 21074147 and 21474129), Science Foundation of Zhejiang Sci-Tech University (14062074-Y), Shanghai Science and Technology Commission (No. 13JC1407000), and Chinese Academy of Sciences.

## Notes and references

<sup>a</sup> Department of Chemistry, Key Laboratory of Advanced Textile Materials and Manufacturing Technology of Education Ministry, Zhejiang Sci-Tech University, Hangzhou 310018, China.

<sup>b</sup> Key Laboratory of Synthetic and Self-assembly Chemistry for Organic Functional Molecules, Shanghai Institute of Organic Chemistry, Chinese Academy of Sciences, 345 Lingling Road, Shanghai 200032, China.

<sup>†</sup> Electronic Supplementary Information (ESI) available: SEM, XPS, TGA, XRD characterization of amino acids capped Cu nanostructure. See DOI: 10.1039/b000000x/

- 1 B. C. Banu, R. Dey, T. Raju and S. Ahammed, *ChemSusChem*, 2017, **5**, 22.
- 2 Z. Liu, J. Xu, D. Chen and G. Shen, *Chem. Soc. Rev.*, 2015, **44**, 161.
- 3 Y. Liu, Z. Liu, N. Lu, E. Preiss, S. Poyraz, M. J. Kim and X. Zhang, *Chem. Commun.*, 2012, **48**, 2621.



- 4 S. Poyraz, Z. Liu, Y. Liu, N. Lu, M. J. Kim and X. Zhang, *Sensors and Actuators B*, 2014, **201**, 65.
- 5 Y. Wei, S. Chen, B. Kowalczyk, S. Huda, T. P. Gray and B. A. Grzybowski, *J. Phys. Chem. C.*, 2010, **114**, 15612.
- 6 Z. Liu, Y. Liu, L. Zhang, S. Poyraz, N. Lu, M. Kim, J. Smith, X. Wang, Y. Yu and X. Zhang, *Nanotechnology*, 2012, **23** 335603.
- 7 D. Zhang, R. Wang, M. Wen, D. Weng, X. Cui, J. Sun, H. Li and Y. Lu, *J. Am. Chem. Soc.*, 2012, **134**, 14283.
- 8 M. P. Pileni, T. Gulik-Krzywicki, J. Tanori, A. Filankembo and J. C. Dedieu, *Langmuir*, 1998, **14**, 7359.
- 9 F. Wang, M. Zhang, Y. Liu and G. Pan, *RSC Adv.*, 2012, **2**, 11235.
- 10 M. Mohl, P. Puzstai, A. Kukovecz and Z. Konya, *Langmuir*, 2010, **26**, 16496.
- 11 Y. Chang, M. Lye and H. Zeng, *Langmuir*, 2005, **21**, 3746.
- 12 A. R. Rathmell, S. M. Bergin, Y. Hua, Z. Li and B. J. Wiley, *Adv. Mater.*, 2010, **22**, 3558.
- 13 A. R. Rathmell and B. J. Wiley, *Adv. Mater.*, 2011, **23**, 4798.
- 14 M. Jin, G. He, H. Zhang, J. Zeng, Z. Xie and Y. Xia, *Angew. Chem. Int. Ed.*, 2011, **50**, 10560.E.
- 15 S. Ye, A. R. Rathmell, Y. Ha, A. R. Wilson and B. J. Wiley, *Small*, 2014, **10**, 1771.
- 16 D. Deng, Y. Jin, Y. Cheng, T. Qi and F. Xiao, *ACS Appl. Mater. Interfaces*, 2013, **5**, 3839.
- 17 S. Jeong, S. H. Lee, Y. Jo, S. S. Lee, Y. Seo, B. W. Ahn, G. Kim, G. Jang, J. Park, B. Ryu and Y. Choi, *J. Mater. Chem. C*, 2013, **1**, 2704.
- 18 Z. Liu, Y. Yang, J. Liang, Z. Hu, S. Li, S. Peng and Y. Qian, *J. Phys. Chem.*, 2003, **107**, 12658.
- 19 D. Mott, J. Galkowski, L. Wang, J. Luo and C.-J. Zhong, *Langmuir* 2007, **23**, 5740.
- 20 Y. Zhao, Z. Zhang, Y. Zhang, Y. Li, Z. He and Z. Yan, *CrystEngComm*, 2013, **15**, 332.
- 21 A. F. Monson and A. T. Woolley, *Nano Lett.*, 2003, **3**, 359.
- 22 A. G. Gelves, Z. T. M. Murakami, M. J. Krantz and J. A. Haber, *Mater. Chem.*, 2006, **16**, 3075.
- 23 H. Wu, L. B. Hu, M. W. Rowell, D. S. Kong, J. J. Cha, J. F. McDonough, J. Zhu, Y. A. Yang, M. D. McGehee and Y. Cui, *Nano Lett.*, 2010, **10**, 4242.
- 24 E. Ye, S. Zhang, S. Liu and M. Han, *Chem. Eur. J.*, 2011, **17**, 3074.
- 25 H. Tung, J. Song, T. Dong, W. Hwang and I. Chen, *Cryst. Growth Des.*, 2008, **8**, 3415.
- 26 J. S. Stevens, A. C. de Luca, M. Pelendritis, G. Terenghi, S. Downes and S. L. M. Schroeder, *Surf. Interface Anal.*, 2013, **45**, 1238.
- 27 Y. Zubavichus, O. Fuchs, L. Weinhardt, C. Heske, E. Umbach, J. Denlinger and M. Grunze, *Radiation Research*, 2004, **161**, 346.
- 28 D. Nolting, E. F. Aziz, N. Ottosson, M. Faubel, I. V. Hertel and J. Winter, *J. Am. Chem. Soc.*, 2007, **129**, 14068.